Large grains matter: contrasting bed stability and morphodynamics during two nearly identical experiments[1]

Lucy G. MacKenzie and Brett C. Eaton

Geography Department, University of British Columbia, Vancouver, BC, Canada

Abstract

While the stabilizing function of large grains in step-pool streams has long been recognized, the role they play in gravel-bed streams is less clear. Most researchers have ignored the role of large grains in gravel bed streams, and have assumed that the median bed surface size controls the erodibility of alluvial boundaries. The experiments presented herein challenge this convention. Two experiments were conducted that demonstrate the significant morphodynamic implications of a slight change to the coarse tail of the bed material. The two distributions had the same range of particle sizes, and nearly identical bulk d_{50} values (1.6 mm), however the d_{90} of experiment GSD1 was slightly finer (3.7 mm) than that for experiment GSD2 (3.9 mm). Transport rates during GSD1 were nearly 4 times greater than during GSD2 (even though the dimensionless shear stress was slightly lower), and the channel developed a sinuous pattern with well developed riffles, pools and bars. During GSD2 the initial channel rectangular channel remained virtually unchanged for the duration of the experiment. The relative stability of GSD2 seems to be associated with a slightly larger proportion of stable (large) grains on the bed surface: at the beginning of GSD1, 3.5% of the bed was immobile, while almost twice as much of it (6.1%) was immobile at the beginning of GSD2. The results demonstrate that the largest grains (not the median size) exert first order control on channel stability.

Keywords:
Physical Modelling, Grain Size Distribution, Gravel-bed Streams, Channel Stability

1. Introduction

Shields' classic work on grain entrainment using a bed of uniform grain sizes is a seminal contribution that strongly influenced the direction of future research in fluvial geomorphology. Shields (1936) concluded that the onset of mobility of particles in a channel occurs when the dimensionless shear stress in a channel exceeds a critical threshold (θ_c). While Shields (1936) found θ_c to be a function of the particle Reynolds number, subsequent researchers found that relative particle exposure (e.g. Fenton and Abbott, 1977) and grain hiding (e.g. Parker et al., 1982) also exert first-order control on the threshold of grain entrainment. Entrainment of bed material can be further modified by the proportion of fine sediment on the bed surface (Ikeda et al., 1988; Wilcock et al., 2001; Venditti et al., 2010), as well as by both channel gradient and relative roughness (Mueller et al., 2005; Bunte et al., 2013; Scheingross et al., 2013; Prancevic and Lamb, 2015).

Investigations of entrainment from a bed composed of a mixture of grain sizes have demonstrated that a wide range of particle sizes are entrained over a narrower range of flows than predicted by Shields' original work (Andrews, 1983; Brayshaw, 1985; Ashworth and Ferguson, 1989). Similarly, full mobility of most sediment sizes in the bed corresponds to the onset of full mobility of the D_{50} (Wilcock and McArdell, 1993, 1997). Such observations have led researchers to conclude that the bed surface D_{50} exerts a first-order control on the entrainment of the entire mixture (Komar, 1987; Parker, 1990; Buffington and Montgomery, 1997), even if true equal mobility of all sediment sizes is seldom if ever observed (Church et al., 1991; Wathen et al., 1995; Lisle, 1995; Parker and Toro-Escobar, 2002).

Researchers have made the logical association between D_{50} mobility and channel form stability. Stable channel geometry has been predicted assuming that the average boundary shear stress is equal to the entrainment threshold

[1] this version of the paper was accepted for publication in Earth Surface Processes and Landforms on January 26, 2017

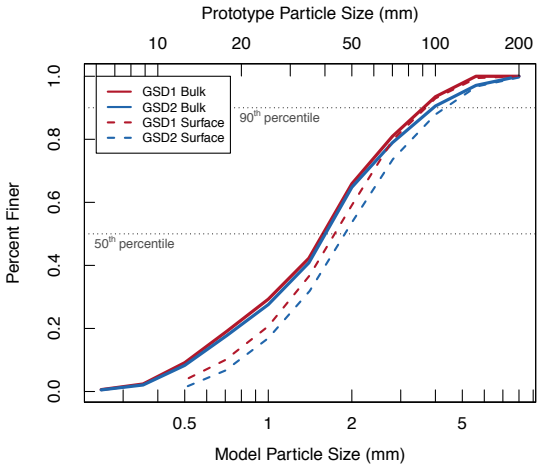

Figure 1: Cumulative percent finer of the GSD of the bulk material and the average surface material. Surface material GSD is truncated at 0.5 mm as this represents the minimum detection limit possible on from the images of the bed. The equivalent prototype grain sizes are indicated by the scale at the top of the figure.

for D_{50} (Li et al., 1976; Parker, 1978; Diplas and Vigilar, 1992), or by estimating the shear stress acting on channel banks and setting that equal to the threshold for D_{50} (Millar and Quick, 1993; Millar, 2005). The surface D_{50} is also incorporated into equations predicting the meandering/braiding threshold (Henderson, 1963; Millar, 2000, 2005; Eaton and Giles, 2009; Eaton et al., 2010), as well as various general frameworks for understanding fluvial mechanics (Andrews, 1984; Parker et al., 1982, 2007). Church (2006) advocates using the Shields parameter as the key variable to distinguish between various channel morphologies, transport characteristics and stabilizing processes. Clearly, there is a great deal of evidence that the D_{50} is a very useful index that captures many essential features of stream morphodynamics.

Some phenomena cannot be explained with reference to the D_{50}. For example, Eaton and Church (2004) identified a threshold channel gradient above which their experimental stream table channels failed to establish and maintain a steady state condition. The only apparent difference between experiments above and below this threshold was a change in the mobility for the largest sizes of sediment in the bed material. Similarly, the initial setup phase of stream table experiments is often plagued by experiments that appear to defy expectations based on Froude scaling of some known prototype; initial trials sometimes exhibit unexpected stability during which bars and pools fail to form, despite their presence in the field prototypes, or they develop an unstable, braided pattern where a stable, single thread pattern is expected. These failures are seldom reported, and are quickly forgotten once the desired behaviour is produced.

This paper presents the results from two stream table experiments that exhibit significant differences in sediment transport characteristics and channel morphology that can only have been caused by the addition of a small amount of coarse sediment to bed material. It is also demonstrated that the observed differences in channel behaviour are inconsistent with the notion that the relative mobility of the median grain size is a suitable index for channel stability.

2. Methods

Two experiments were conducted using the Adjustable-Boundary Experimental System (A-BES) at the University of British Columbia. A-BES comprises a 1.5 m wide by 12.2 m long tilting stream table with a computerized instrument cart that uses a laser scanning system to collect 2 mm resolution digital elevation models (DEMs) of the bed. The experiments are generic Froude-scaled models based on field measurements from steep gravel-bed streams in Alberta, Canada. Using a length scale ratio of 1:25, they represent a prototype channel with a bankfull width of 10 m, a mean channel gradient of 0.02 m/m and a bankfull flow of approximately 2 m^3/s.

Bulk grain size distributions measured in the field were used to develop the model sediment mixtures (see Figure 1); the distributions are typical of gravel bed streams, and are similar to that used by Eaton and Church (2004). In

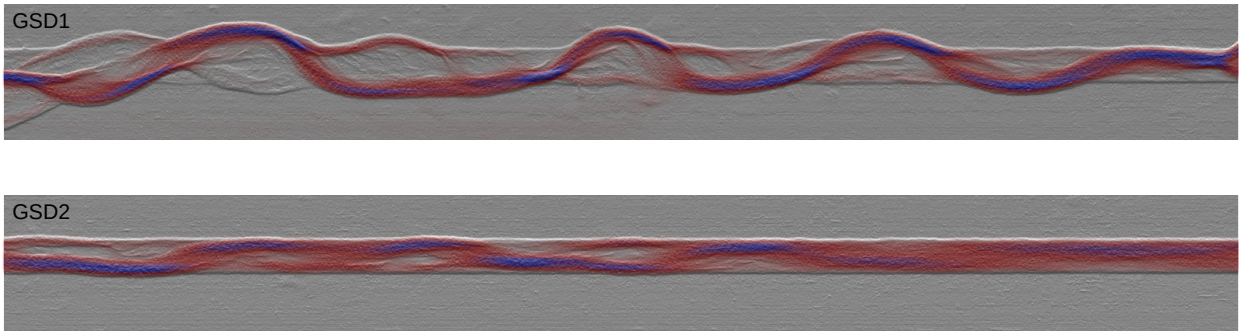

Figure 2: Specific discharge shown for the two experiments at 8 hrs. Flow from right to left.

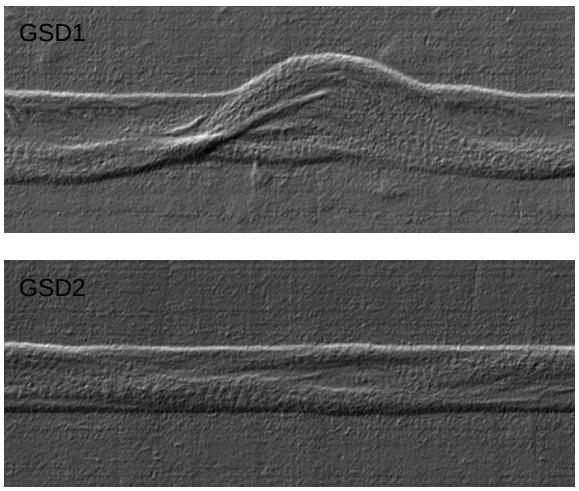

Figure 3: Detail of hillshaded DEM at 8 hrs.

order to maintain a hydraulically rough boundary, the model sediment mixture does not include sediment finer than 0.25 mm, and corresponds to a field sediment distribution truncated at 6.25 mm.

Two slightly different bed material grain size distributions were used for Experiment GSD1 and Experiment GSD2; in all other respects, the experiments were identical. The first experiment (GSD1) was conducted using a bulk grain size distribution for which d_{50} = 1.60 mm, d_{90} = 3.67 mm, and d_{95} = 4.37 mm. For the second experiment (GSD2) additional coarse material ranging in size from 4 to 8 mm was added to GSD1, producing a distribution for which d_{50} = 1.63 mm, d_{90} = 3.94 mm, and d_{95} = 5.09 mm. Both grain size distributions are consistent with the range of distributions measured in the field.

The experiments were started in a straight, unarmoured, 30 cm wide and 1.5 cm deep channel, and were run for a total of 8 hrs at a discharge of 0.7 L/s with no sediment feed. Flow was stopped every hour in order to scan the bed and collect images of the bed surface. Digital Elevation Models (DEMs) of the bed were smoothed using a 7 x 7 pixel averaging filter, and a 15 x 15 pixel averaging filter was used to fill in any missing data. Photos of the coarsest portion of the channel were taken at five locations along the stream table, and used to estimate the bed surface texture using a grid-by-number sampling approach (Bunte and Abt, 2001); each photo represented an area of approximately 30 cm by 20 cm. Sediment output from the stream table was collected at 15 min intervals using a trap with a mesh of 0.25 mm. Samples were dried, weighed and combined into 30 min samples for grain size analysis.

Because it is difficult to measure flow depth and velocity in stream table experiments due to the shallow depths ($Y \approx 0.005$ m) and a rapidly evolving channel bed (see time lapse video in the supplementary material), the flow conditions (water depth, velocity, shear stress) were reconstructed by applying a 2D numerical flow model (Nays2DH)

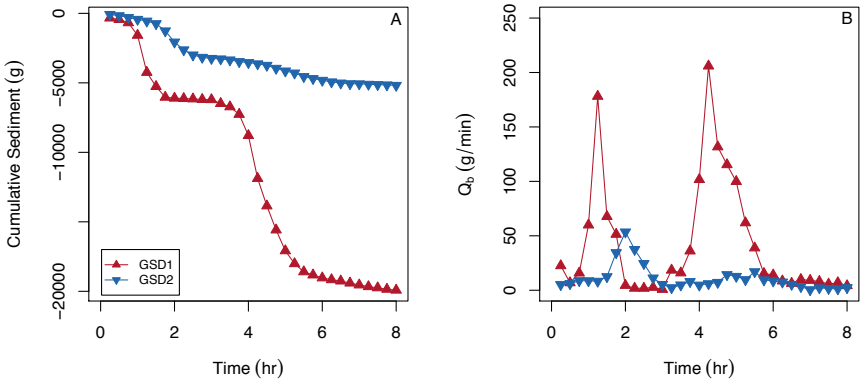

Figure 4: A) Cumulative sediment output; B) Bedload transport rate through time

to the hourly bed surface DEMs. To minimize rounding errors associated with the magnitude of depths being simulated and the size of the grid, the DEM size and discharge were adjusted to prototype scale (i.e. using a length scale of 25) for the flow modelling. The estimated water depths, shear stresses and velocities from Nays2DH were then back-transformed to the model scale. When parameterizing the Nays2DH models, we specified reach-averaged Manning's n values determined using the flow resistance law presented by Ferguson (2007). The results of the flow model were qualitatively validated by overlaying maps of specific discharge (Figure 2) onto downlooking images of the bed taken during the run. The extent of the modelled wetted areas agrees well with the observed wetted area during the runs. In any case, only the reach-average shear stress values are used in this analysis on the grounds that local variations in bed roughness can affect the spatial distribution of shear stress but are not likely to have a significant effect on the reach average values.

3. Results

Experiments GSD1 and GSD2 exhibited very different morphodynamics (see video in supplementary material). GSD1 developed a sinuous channel with distinct bars, riffles and pools. GSD2 remained straight, and only developed low-amplitude bars (Figures 2 and 3). The reach-average channel geometry at the end of the experiments varied markedly, as well. At the end of GSD1, the average channel width (W) and depth (Y) were 0.65 m and 0.005 m, respectively, while for GSD2, the values were 0.36 m and 0.008 m, respectively.

Both GSD1 and GSD2 experienced net degradation, since there was no sediment feed at the upstream end of the stream table. The total volume of degradation during GSD1 (19916 g) was nearly four times the total during GSD2 (5183 g) (Figure 4A). The sediment output rate during GSD1 fluctuated over several orders of magnitude, reaching peak output rates of 178 and 206 g/min at 1 hr and 5 hrs, respectively (Figure 4B). In contrast, the output rate during GSD2 reached a maximum of 54 g/min at 2 hrs, and was less variable over the course of the experiment.

During GSD1, degradation resulted primarily from lateral erosion and evacuation of bank material (Figure 5). In fact, most areas within the original templated channel experienced net aggradation, raising the local bed elevation. During GSD2, almost no bank erosion occurred and the relatively small loss of sediment that did occur resulted from vertical scour. During the last 2 hrs of both experiments, the channels became nearly static, and the average sediment output rate was less than 10 g/min.

While bedload sediment texture did vary over the course of GSD1 and GSD2, the temporal trends were not significant, based on the p-values for the regression coefficients presented in Table 1. Despite slightly different bed material distributions, the distribution of the transported load was nearly identical for the two experiments. The range of values for the bedload median size (L_{50}) and the 90th percentile (L_{90}) are shown in Figure 6A; the mean values of L_{50} and L_{90} are not statistically different for GSD1 and GSD2 at the 95% confidence level (Table 2).

The bed surface texture coarsened over time during both experiments (Figure 7), though the trends for D_{50} and D_{90} are not statistically significant for GSD1 (Table 1). The bed surface developed during GSD2 was slightly coarser than that which developed during GSD1 (Figure 1) as both D_{50} and the D_{90} for GSD2 were statistically larger than

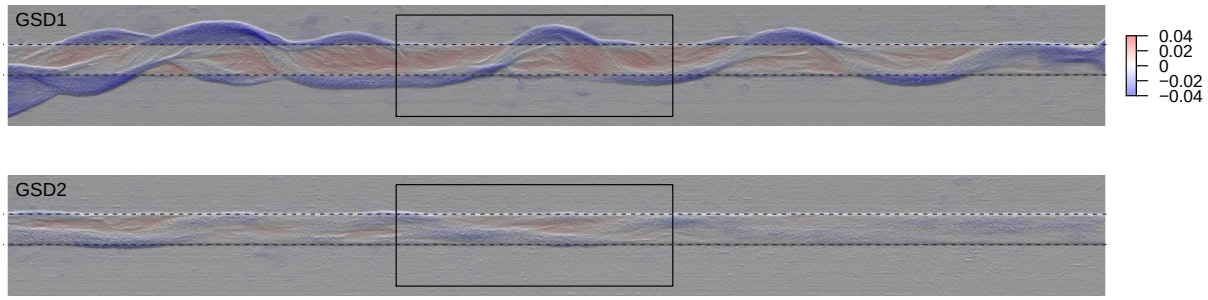

Figure 5: DEMs of difference for the two experiments. Flow from right to left. Dashed lines show initial templated channel bank locations. Values in legend represent a difference in elevation given in meters. Solid-line boxes highlight area plotted in Figure 3.

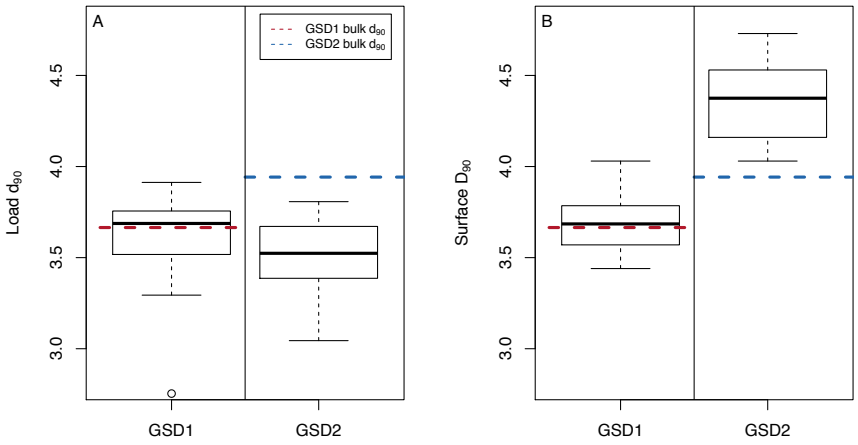

Figure 6: Load and surface grain sizes for the two experiments.

Table 1: Linear regression results for temporal trends in bedload and bed surface grain size distributions.

Linear Regression	Equation	R^2	P [a]
Time ~ GSD1 L_{50}	$y = -0.0119x + 1.797$	0.0831	0.2976
Time ~ GSD1 L_{90}	$y = -0.0211x + 3.688$	0.0294	0.5415
Time ~ GSD2 L_{50}	$y = -0.0054x + 1.759$	0.0289	0.5294
Time ~ GSD2 L_{90}	$y = 0.0344x + 3.347$	0.1210	0.1868
Time ~ GSD1 D_{50}	$y = 0.0389x + 1.593$	0.4794	0.0570
Time ~ GSD1 D_{90}	$y = 0.0361x + 3.531$	0.2314	0.2276
Time ~ GSD2 D_{50}	$y = 0.0492x + 1.708$	0.8807	**5.56e-04**
Time ~ GSD2 D_{90}	$y = 0.0808x + 3.998$	0.6548	**5.11e-08**

[a] $P < 0.05$ indicates a statistically significant trend, shown in **bold**.

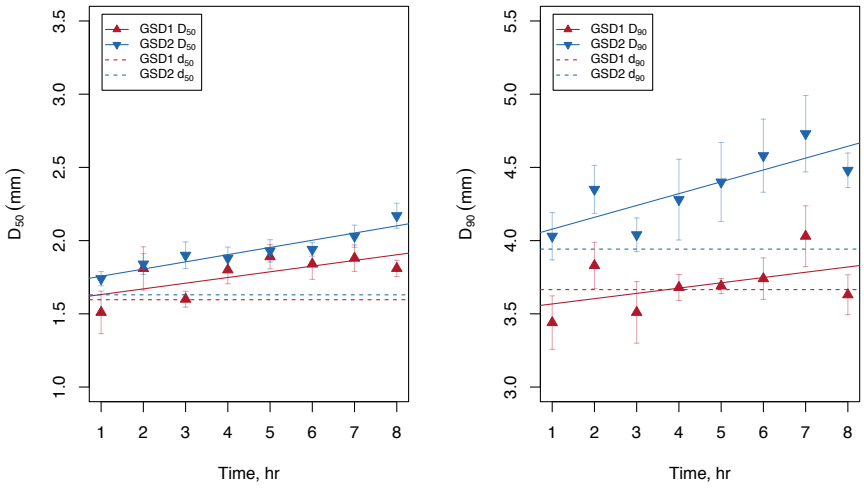

Figure 7: Mean surface D_{50} and D_{90} through time for the two experiments. The solid lines represent the results of linear regressions conducted on these mean values (Equations and R-squared values presented in Table 1). Whiskers show the standard error of the mean (n = 5).

the values for GSD1 (Figure 6B; Table 2). Excluding data from the first hour of the experiment, the armour ratio calculated from the surface D_{50} and the subsurface bulk d_{50} varied from about 1.00 to 1.18 for GSD1, and from about 1.10 to 1.25 for GSD2 (Table 3). These armour ratios are lower than they would be in the field prototype, since the model grain size distribution is truncated at 0.25 mm (equivalent to 6.25 mm in the prototype). If it is assumed that approximately 25% of the bulk sediment for the prototype is finer than this limit and that there would be virtually none of this sediment size on the bed surface, the bulk d_{50} would be about 0.93 mm for GSD1, giving armour ratios ranging from 1.72 to 2.03, which is close to the typical values for this kind of gravel bed stream.

Table 2: T-test results comparing different grain size distribution metrics.

T-Test	$\bar{X}_1$	$\bar{X}_2$	t [a]
GSD1 L_{50} ~ GSD2 L_{50}	1.75	1.74	0.284
GSD1 L_{90} ~ GSD2 L_{90}	3.60	3.49	1.067
GSD1 D_{50} ~ GSD2 D_{50}	1.77	1.93	**-2.427**
GSD1 D_{90} ~ GSD2 D_{90}	3.69	4.36	**-6.171**

[a] negative t values indicates $\bar{X}_1 < \bar{X}_2$. Statistically significant differences are shown in **bold**.

The flow modelling results indicate differences in the reach average flow conditions resulting from the different bed morphologies developed during GSD1 and GSD2. The distribution of τ is not a simple, normal distribution, because extensive areas of the channel bed during GSD1 were covered by slow moving, shallow water, which dramatically reduces the reach-average shear stress (Figure 8). During the first hour, both GSD1 and GSD2 saw a decrease in reach-averaged shear stress (τ) from that associated with the initial channel (for which τ = 2.2 Pa). The magnitude of change was greater in the GSD1 experiment and τ continued to decrease until 3 hrs, at which point it stabilized at approximately 0.95 Pa. In the GSD2 experiment, τ dropped to 1.68 Pa during the first hour and remained at about this value for the rest of the experiment.

In order to make a more meaningful comparison of the shear stresses in the main channel around the thalweg, the median shear stress (τ_{50}) was estimated for a flow field that excludes data from grid cells for which $q < 0.0005$ m^2/s. An estimate of the 95th percentile of the shear stress distribution in the main channels (τ_{95}) was also used as an index of the upper range of the shear stress distributions. The values of τ_{50} and τ_{95} are presented in Table 4. For GSD1, the values of τ_{50} oscillated about a mean value of approximately 1.6 ± 0.013 Pa, while they varied about a mean of 1.9 ± 0.024 Pa for GSD2. This comparison implies that the typical bed shear stresses during GSD2 were systematically greater than those acting on the bed during GSD1, though the differences (in the main channel, at least) are not as

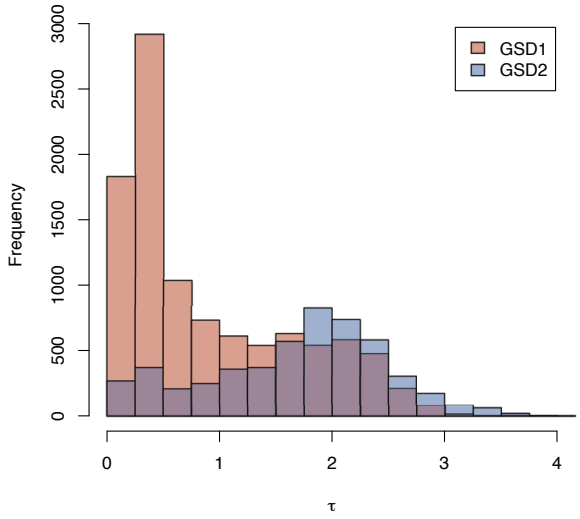

Figure 8: Histograms of shear stress values for Experiments GSD1 and GSD2 based on Nays2DH modelling using the bed topography after 8 hrs. The histogram presents the number of grid cells having shear stress values in a particular range, and the sum of all columns is proportional to the total area covered by flowing water.

large as estimates of the mean reach-average τ would suggest. The difference in the maximum bed shear stresses for the two experiments is not as large; the values of τ_{95} for GSD1 and GSD2 varied about mean values of 2.6 ± 0.011 Pa and 2.7 ± 0.041 Pa, respectively, suggesting that the peak bed shear stresses were approximately the same in both experiments.

Using the value of τ_{50} estimated for the main channel and the value of D_{50} (which is based on photos of approximately the same part of the channel), the Shields number (θ_{50}) was estimated as follows:

$$\theta_{50} = \frac{\tau_{50}}{g(\rho_s - \rho)D_{50}} \tag{1}$$

For GSD1, θ_{50} varies from 0.052 to 0.065 with a mean value of 0.056. For GSD2, θ_{50} varies from 0.059 to 0.066 with a mean of 0.063. Not only are the shear stresses higher for GSD2, the θ_{50} is slightly higher, too. However, despite the higher θ_{50} values during GSD2, the channel was much less active and the sediment transport rates were much lower, relative to GSD1.

4. Discussion

These experiments demonstrate that the median surface grain size does not control channel stability. Traditional approaches for predicting the threshold for channel change compare the reach-averaged dimensionless shear stress (θ_{50}) to the entrainment threshold for the D_{50} (e.g., Li et al., 1976; Parker, 1978; Diplas and Vigilar, 1992; Millar and Quick, 1993). The current consensus on stream channel dynamics predicts that channel change should occur when θ_{50} exceeds some critical value, with the magnitude of the changes proportional to the degree to which the threshold is exceeded. This idea appears to be fundamentally incorrect, since the experiment with the higher θ_{50} remained stable while the one with the lower value widened, developed a sinuous, riffle pool morphology and transported four times as much bed material. The results from this study suggest that the largest grains in the bed material control channel stability.

While some researchers have noted the importance of coarse material in bar stabilization (Leopold and Wolman, 1957; Lewin, 1976; Lisle et al., 1991), others have ignored the issue, conducting experiments that use very narrowly graded sediments to explore bar dynamics (Jaeggi, 1984; Ikeda, 1984; Termini, 2009), which eliminates the potential effects described herein. Furthermore, the traditional use of fixed-wall flumes (e.g. Lewin, 1976; Ikeda, 1984; Lisle et al., 1991; Lanzoni, 2000; Termini, 2009) to study sediment transport and bedform dynamics make it impossible

Table 3: Sediment properties table

		Output Rate	Load (mm)			Surface (mm)		
	Hour	(g/min)	L_{50}	L_{90}	L_{95}	D_{50}	D_{90}	D_{95}
GSD1	1	26.3	1.75	3.65	4.24	1.51	3.44	3.82
	2	75.4	1.76	3.89	4.66	1.81	3.83	4.92
	3	1.8	1.50	2.75	3.43	1.60	3.51	3.94
	4	43.0	1.77	3.51	4.06	1.80	3.68	4.11
	5	138.2	1.78	3.77	4.47	1.89	3.69	4.14
	6	32.5	1.78	3.67	4.18	1.84	3.74	4.44
	7	8.5	1.69	3.54	4.00	1.88	4.03	4.76
	8	6.2	1.66	3.36	3.88	1.81	3.63	4.31
GSD2	1	7.2	1.80	3.55	3.98	1.74	4.03	4.89
	2	27.2	1.82	3.57	4.05	1.84	4.35	5.49
	3	19.7	1.64	3.07	3.67	1.90	4.04	4.91
	4	5.0	1.64	3.25	3.81	1.88	4.28	5.14
	5	10.1	1.74	3.51	4.00	1.84	4.42	5.20
	6	11.2	1.74	3.60	4.13	1.78	4.48	5.64
	7	4.2	1.72	3.71	4.48	2.03	4.73	5.78
	8	1.9	1.80	3.70	4.32	1.98	4.01	5.40

Table 4: Hydraulic properties table

	Hour	W (m)	Y (m)	τ_{50} (Pa)	τ_{95} (Pa)	A_f (m^2)
GSD1	0	0.30	0.0110	2.12	2.92	3.78
	1	0.44	0.0070	1.60	2.63	3.77
	2	0.61	0.0056	1.55	2.53	3.86
	3	0.66	0.0053	1.53	2.53	3.76
	4	0.64	0.0054	1.56	2.61	3.73
	5	0.62	0.0055	1.65	2.73	3.55
	6	0.65	0.0054	1.59	2.61	3.64
	7	0.67	0.0053	1.59	2.58	3.72
	8	0.68	0.0052	1.58	2.53	3.71
GSD2	0	0.30	0.0113	2.23	3.10	3.87
	1	0.35	0.0088	1.86	2.51	3.74
	2	0.36	0.0088	1.89	2.74	3.69
	3	0.36	0.0087	1.87	2.66	3.69
	4	0.36	0.0088	1.89	2.72	3.69
	5	0.36	0.0089	1.92	2.77	3.67
	6	0.36	0.0088	1.90	2.79	3.66
	7	0.36	0.0091	1.96	2.89	3.71
	8	0.36	0.0088	1.89	2.83	3.67

Note: the values τ_{50} and τ_{95} were calculated for a flow field including only grid cells with $q > 0.0005$ m^2/s to facilitate comparison of the stresses acting in the main channel near the thalweg for both experiments. The total bed area (A_f) for which $q > 0.0005$ m^2/s is similar for GSD1 and GSD2

to study channel stability, since channel width and slope are fixed quantities, rather than adjustable properties of the system, as they are in the field. It is only in stream table experiments (or in the field) that the full suite of processes controlling channel stability can be studied, which perhaps explains why the scientific community has failed to make a distinction between sediment mobility (comprising the entrainment and transport of grains) and sediment stability (involving the interactions between large bed particles, the near-bed flow structure, and other bed particles).

For the two experiments studied herein, most of the channel adjustments took place during the first hour. By the second hour, bed shear stress, wetted width, and depth reached reasonably stable values. While θ_{50} is different for the two experiments, the Shields number calculated using the D_{95} is approximately the same for both GSD1 and GSD2, having an average of 0.022 (excluding data from the first hour), which is consistent with the entrainment threshold of 0.02 for large grains, reported by Andrews (1983). This suggests that, after the initial period of bank erosion, bed deformation, bar deposition and/or surface coarsening during the first hour, both experiments reached a stable state defined by the threshold of motion for the largest grains on the bed, despite consistently different θ_{50} values.

Although the stable channels developed by the end the experiments are both consistent with a threshold channel associated with the largest grains, the processes producing the threshold state were quite different. Despite the lower θ_{50} values during GSD1, erosion of channel banks during that experiment triggered a feedback mechanism between channel form and local transport capacity that led to the development of a sinuous channel with a riffle-pool morphology, ultimately resulting in a wider, shallower channel. This lateral instability also supplied the system with sediment via extensive bank erosion, such that much of the initial channel was subject to local net aggradation (GSD1 in Figure 5). In contrast, during GSD2, the initial channel degraded and coarsened, and did not receive any significant sediment inputs due to lateral channel migration. In this circumstance, only low amplitude, poorly developed bars formed (Figure 5). In light of this, the explanation for such different response trajectories must relate to the initial mobility of the largest grains, and through that, the capacity of the channel to erode its banks.

At the beginning of both experiments, τ_{50} was approximately 2.2 Pa (see Table 4). Assuming that the bed surface initially had the same median size as the bulk sediment distribution, the values of τ_{50} were 0.082 and 0.085 for GSD1 and GSD2, respectively. According to these calculations and considering the relatively unstructured and unarmored state of the channel bed at the beginning of the experiments, the bed surface D_{50} should have been fully mobile and both channels should have been laterally active. Previous work summarized by Lisle et al. (1991) suggests that alternate bars should form for these conditions, as well. Nevertheless, the experiment with the slightly higher τ_{50} value (GSD2) remained laterally stable and did not develop a well defined set of alternate bars, whereas that with the lower value deformed its boundaries and developed a sinuous planform with prominent bars, pools and riffles. The processes governing channel stability can clearly not be associated with mobility of the D_{50} at a fundamental level, even if mobility of the D_{50} is a useful index. The D_{50} does not control channel stability.

If the D_{50} is not controlling channel stability, then what is controlling it? An analysis of relative mobility using the ratio of the bedload sediment size (L_i) to the bed surface sediment size (D_i) indicates that the largest grains in the bed material were systematically underrepresented in the load for GSD2 (but not GSD1), suggesting that they were only partially mobile (Figure 9). Assuming that full mobility corresponds to L_i/D_i ratios of between 0.85 and 1.15, the bed surface D_{50}, D_{90} and D_{95} were all fully mobile for the duration of GSD1. However, for GSD2, the bed surface D_{50} was fully mobile, but the larger size classes (i.e. D_{90} and D_{95}) were not.

Perhaps the difference between the morphodynamics of GSD1 and GSD2 can be associated with the areal concentration of stable grains on the bed surface. According to Wilcock and McArdell (1997), grains in a given size class become partially mobile once shear stress of the bed exceeds the critical Shields number and become fully mobile at twice the critical Shields number. However, not all partially mobile grains contribute to channel stability (i.e., some of those grains will have moved during the experiment). Work by Wilcock and McArdell (1997) suggests that, for a size class at the threshold between stability and partial mobility (i.e., $\tau = \tau_{ci}$, where τ_{ci} is the critical shear stress to entrain that size class), 90% of the grains on the bed within that class will remain immobile; in contrast, for a size class at the threshold between partial mobility and full mobility (i.e., $\tau = 2\tau_{ci}$), only 10% of the grains on the bed will remain immobile. Assuming that the proportion of immobile grains on the bed decreases linearly as τ increases from $\tau = \tau_c$ to $\tau = 2\tau_c$, it is estimated that $3.5 \pm 1\%$ of the initial bed surface was immobile during GSD1 and $6.1 \pm 1\%$ of the initial bed was immobile during GSD2 (the estimated error is based on uncertainty for the bed surface texture values). By the end of the experiments (when both channels had achieved a stable configuration), it is estimated that the proportion of the bed that was stable had increased for both experiments, reaching statistically similar values ($12 \pm 1\%$ for GSD1 and $13 \pm 1\%$ for GSD2).

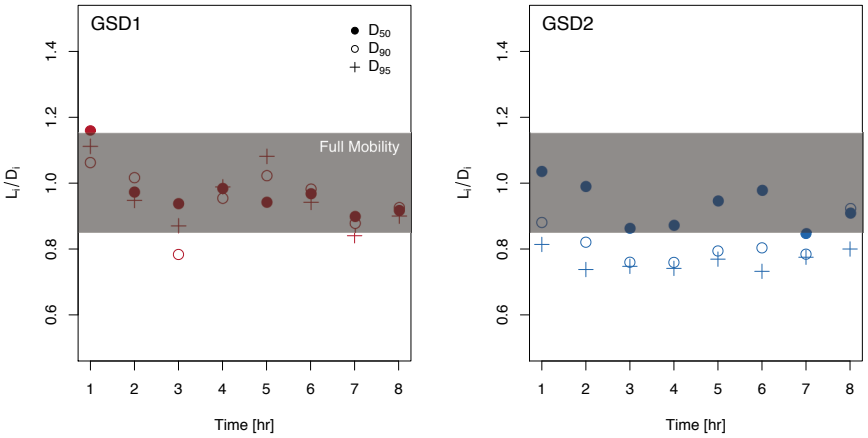

Figure 9: The ratio of the texture of the transported material to the bed surface is shown for the median (solid circles), the 90th percentile (open circles) and the 95th percentile (plus signs) of each distribution for GSD1 (red) and GSD2 (blue).

These results suggest that: (1) for channel planform to be stable (in the presence of bed material transport), approximately 5% of the bed must be immobile; and (2) for a channel to reach a static state (i.e. having both a stable channel pattern and experiencing transport rates close to zero) approximately 10% of the bed must be immobile. While it may seem that an immobility threshold of 5% is small, this value is comparable to the results reported by Gao et al. (2016), who found that aeolian dunes do not form when the initial proportion of coarse (i.e. immobile) grains within the bed is greater than 4-5%. While more work remains to be done to explore the mechanisms by which these coarse grains stabilize a surface, there is strong evidence to suggest that small changes to the coarse tail of a deposit can play a significant role in altering the morphodynamics of a sedimentary surface.

The realization that small changes to the coarse end of the bed material grain size distribution can significantly alter the channel dynamics has potentially important implications for stream restoration. In some circumstances it is desirable to increase the level of channel stability without imposing hard engineering solutions, such as in urban streams where peak flows have been increased and the channel has been de-stabilized. In other circumstances, stream managers are attempting to restore natural channel dynamics in regulated streams where dams have significantly reduced the available peak flows, resulting in channels that are no longer capable of eroding their banks, building bars or scouring pools. The results of this work suggest that channel stability can be significantly modified by adding or removing a small fraction of the bed material from the coarse tail of the distribution. It is therefore possible that restoration approaches that either augment or reduce the proportion of coarse sediment in the bed material could be used to restore streams in the situations described above.

5. Conclusions

The results of two identical experiments conducted with nearly identical bed material distributions demonstrate an incomplete understanding of the factors controlling channel stability. The experiments suggest that channel stability is most likely controlled by the largest grains on the bed surface, which remain immobile even during flood events; stability does not seem to be controlled by the median surface grain size, which is fully mobile during floods. It was found that adding a relatively small volume of coarse sediment to the bed material (which produced only a 15% increase of the d_{95} of the bulk material) resulted in a 48% decrease in channel width and a 75% decrease in average sediment transport rate. The addition of coarse material also produced a transition from a lateral style of channel adjustment, in which bank erosion allows for the development of a sinuous channel and pool-riffle morphology, to a primarily vertical style of adjustment involving essentially no bank erosion. Given the design of the models used in these experiments, results from this study are strictly applicable to relatively small, sediment supply limited threshold channels. However, observations from numerous related experiments using the same grain size distributions seem to confirm that large grain sizes control channel stability over a wide range of discharge values and sediment supply

rates. Forthcoming work based on these additional experiments will further explore the processes by which large grain act to stabilize channel morphology.

Acknowledgements

The idea for these experiments comes from discussions of a series of experimental trials during a collaborative project with Laura Hempel, Marwan Hassan and Gordon Grant, and we are grateful for the stimulating discussions this collaboration produced. The paper also benefited from numerous conversations about the experiments at the 2016 American Geophysical Union Fall Meeting with experts in the field too numerous to count; we appreciate the support and the challenging questions put to us at that meeting, and we feel this paper has been much improved as a result. Finally, the paper was very carefully and critically reviewed by two anonymous reviewers who dramatically improved the paper by challenging us to put our arguments more clearly and to more explicitly identify the novelty of our findings.

References

Andrews, ED., 1983. Entrainment of gravel from naturally sorted riverbed material. Geological Society of America Bulletin **94**: 1225–1231. DOI: 10.1130/0016-7606(1983)94<1225:EOGFNS>2.0.CO;2.

Andrews, ED. 1984. Bed-material entrainment and hydraulic geometry of gravel-bed rivers in Colorado. *Geological Society of America Bulletin* **95**: 371–378. DOI: 10.1130/0016-7606(1984)95<371:BEAHGO>2.0.CO;2

Ashworth, PJ, Ferguson, RI. 1989. Size-selective entrainment of bed-load in gravel bed streams. *Water Resources Research* **25**: 627–634. DOI: 10.1029/WR025i004p00627

Brayshaw, AC. 1985. Bed microtopography and entrainment thresholds in gravel-bed rivers. *Geological Society of America Bulletin* **96**: 218–223. DOI: 10.1130/0016-7606(1985)96<218:BMAETI>2.0.CO

Buffington, JM, Montgomery, DR. 1997. A systematic analysis of eight decades of incipient motion studies, with special reference to gravel-bedded rivers. *Water Resources Research* **33**: 1993–2029. DOI: 10.1029/97WR03138

Bunte, K, Abt, S. 2001. *Sampling surface and subsurface particle-size distributions in wadable gravel- and cobble-bed streams for analyses in sediment transport, hydraulics, and streambed monitoring*. General Technical Report RMRS-GTR-74. USDA Forest Service, Rocky Mountain Research Station.

Bunte, K, Abt, SR, Swingle, KW, Cenderelli, DA, Schneider, JM. 2013. Critical Shields values in coarse-bedded steep streams. *Water Resources Research* **49**: 7427–7447. DOI: 10.1002/2012WR012672

Church, M. 2006. Bed material transport and the morphology of alluvial river channels. *Annual Review of Earth and Planetary Sciences* **34**: 325–354. DOI: 10.1146/annurev.earth.33.092203.122721

Church, M, Wolcott, JF, Fletcher, WK. 1991. A test of equal mobility in fluvial sediment transport: behavior of the sand fraction. *Water Resources Research* **27**: 2941–2951. DOI: 10.1029/91WR01622

Diplas, P, Vigilar, GG, 1992. Hydraulic geometry of threshold channels. *Journal of Hydraulic Engineering* **118**: 597–614. DOI: 10.1061/(ASCE)0733-9429(1992)118:4(597)

Eaton, BC, Church, M. 2004. A graded stream response relation for bed load-dominated streams. *Journal of Geophysical Research* **109**. DOI: 10.1029/2003JF000062

Eaton, BC, Church, M, Millar, RG, 2004. Rational regime model of alluvial channel morphology and response. *Earth Surface Processes and Landforms* **29**: 511–529. DOI: 10.1002/esp.1062

Eaton, BC, Giles, TR. 2009. Assessing the effect of vegetation-related bank strength on channel morphology and stability in gravel-bed streams using numerical models. *Earth Surface Processes and Landforms* **34**: 712–724. DOI: 10.1002/esp

Eaton, BC, Moore, RD, Giles, TR. 2010. Forest fire, bank strength and channel instability: the 'unusual' response of Fishtrap Creek, British Columbia. *Earth Surface Processes and Landforms* **35**: 1167–1183. DOI: 10.1002/esp.1946

Fenton, JD, Abbott, JE. 1977. Initial movement of grains on a steam bed: the effect of relative protusion. *Proceedings of the Royal Society of London ser.* **352**: 523–537. DOI: 10.1098/rspa.1977.0014

Ferguson, RI. 2007. Flow resistance equations for gravel- and boulder-bed streams. *Water Resources Research* **43**: 0–12. DOI: 10.1029/2006WR005422

Gao, X, Narteau, C, Rozier, O, 2016. Controls on and effects of armoring and vertical sorting in aeolian dune fields: a numerical simulation study. Geophysical Research Letters **43**: 2614–2622. DOI: 10.1002/2016GL068416

Henderson, FM. 1963. Stability of alluvial channels. *Transactions of the American Society of Civil Engineers* **128**: 657–686.

Ikeda, S. 1984. Prediction of alternate bar wavelength and height. Journal of Hydraulic Engineering **110**: 371–386. DOI: 10.1061/(ASCE)0733-9429(1984)110:4(371)

Ikeda, S, Parker, G, Kimura, Y. 1988. Stable width and depth of straight gravel rivers with heterogeneous bed materials. *Water Resources Research* **24**: 713–722. DOI: 10.1029/WR024i005p00713

Jaeggi, M., 1984. Formation and effects of alternate bars. Journal of Hydraulic Engineering **110**: 142–156. DOI: 10.1061/(ASCE)0733-9429(1984)110:2(142)

Komar, PD. 1987. Selective gravel entrainment and the empirical evaluation of flow competence. *Sedimentology* **34**: 1165–1176. DOI: 10.1111/j.1365-3091.1987.tb00599.x

Lanzoni, S. 2000. Experiments on bar formation in a straight flume: 1. Uniform sediment. Water Resources Research **36**: 3337–3349. DOI: 10.1029/2000WR900161

Leopold, L. B., Wolman, M. G., 1957. River channel patterns: braided, meandering and straight. Physiography and Hydraulic Studies of Rivers *Geological Survey Professional Paper 282-B*: 39–85.

Lewin, J. 1976. Initiation of bedforms and meanders in coarse-grained sediment. Geological Society of America Bulletin **87**: 281–285. DOI: 10.1130/0016-7606(1976)87<281:IOBFAM>2.0.CO;2

Li, R-M, Stevens, MA, Simons, DB. 1976. Morphology of cobble streams in small watersheds. *Journal of the Hydraulics Division* **102**: 1101–1117.

Lisle, TE. 1995. Particle size variation between bedload and bed material in natural gravel beds channel. *Water Resource Research* **31**: 1107–1118. DOI: 10.1080/10106049809354637

Lisle, TE, Ikeda, H, Iseya, F. 1991. Formation of stationary alternate bars in a steep channel with mixed-size sediment: A flume experiment. Earth Surface Processes and Landforms **16**: 463–469. DOI: 10.1002/esp.3290160507

Millar, RG. 2000. Influence of bank vegetation on alluvial channel patterns. *Water Resources Research* **36**: 1109–1118. DOI: 10.1029/1999WR900346

Millar, RG. 2005. Theoretical regime equations for mobile gravel-bed rivers with stable banks. *Geomorphology* **64**: 207–220. DOI: 10.1016/j.geomorph.2004.07.001

Millar, RG, Quick, M. 1993. Effect of bank stability on geometry of gravel rivers. *Journal of Hydraulic Engineering* **119**: 1343–1363. DOI: 10.1061/(ASCE)0733-9429(1993)119:12(1343)

Mueller, ER, Pitlick, J, Nelson, JM. 2005. Variation in the reference Shields stress for bed load transport in gravel-bed streams and rivers. *Water Resources Research* **41**: DOI: 10.1029/2004WR003692

Parker, G., 1978. Self-formed straight rivers with equilibrium banks and mobile bed. Part 2. The gravel river. *Journal of Fluid Mechanics* **89**: 127–146. DOI: 10.1017/S0022112078002505

Parker, G. 1990. Surface-based bedload transport relation for gravel rivers. *Journal of Hydraulic Research* **28**: 417–436. DOI: 10.1080/00221689009499058

Parker, G, Klingeman, PC, McLean, DG. 1982. Bedload and size distribution in paved gravel-bed streams. *Journal of the Hydraulics Division* **108**: 544–571. DOI: 10.1061/(ASCE)0733-9429(1983)109:5(793)

Parker, G, Toro-Escobar, CM. 2002. Equal mobility of gravel in streams: the remains of the day. *Water Resources Research* **38**: 1–8. DOI: 10.1029/2001WR000669

Parker, G, Wilcock, PR, Paola, C, Dietrich, WE, Pitlick, J. 2007. Physical basis for quasi-universal relations describing bankfull hydraulic geometry of single-thread gravel bed rivers. *Journal of Geophysical Research* **112**. DOI: 10.1029/2006JF000549

Prancevic, JP, Lamb, MP. 2015. Unraveling bed slope from relative roughness in initial sediment motion. *Journal of Geophysical Research: Earth Surface* **120**. DOI: 10.1002/2014JF003323

Scheingross, JS, Winchell, EW, Lamb, MP, Dietrich, WE. 2013. Influence of bed patchiness, slope, grain hiding, and form drag on gravel mobilization in very steep streams. *Journal of Geophysical Research: Earth Surface* **118**: 982–1001. DOI: 10.1002/jgrf.20067

Shields, A. 1936. *Application of similarity principles and turbulence research to bed-load movement*, WM Keck Laboratory of Hydraulics and Water Resources Report 167 (Translated from German by WP Ott and JC van Uchelen, California Institute of Technology, Pasadena, CA).

Termini, D. 2009. Experimental observations of flow and bed processes in large-mmplitude meandering flume. Journal of Hydraulic Engineering **135**: 575–587. DOI: 10.1061/(ASCE)HY.1943-7900.0000046

Venditti, JG, Dietrich, WE, Nelson, PA, Wydzga, MA, Fadde, J. Sklar, L. 2010. Mobilization of coarse surface layers in gravel-bedded rivers by finer gravel bed load. *Water Resources Research* **46**: 1–10. DOI: 10.1029/2009WR008329

Wathen, SJ, Ferguson, RI, Hoey, TB, Werritty, A. 1995. Unequal mobility of gravel and sand in weakly bimodal river sediments. *Water Resources Research* **31**: 2087–2096. DOI: 10.1029/95WR01229

Wilcock, P, Kenworthy, S, Crowe, J. 2001. Experimental study of the transport of mixed sand and gravel. *Water Resources Research* **37**: 3349–3358. DOI: 10.1029/2001WR000683

Wilcock, PR, McArdell, BW. 1993. Surface-based fractional transport rates: mobilization thresholds and partial transport of a sand-gravel sediment. *Water Resources Research* **29**: 1297–1312. DOI: 10.1029/92WR02748

Wilcock, PR, McArdell, BW. 1997. Partial transport of a sand/gravel sediment. *Water Resources Research* **33**: 235. DOI: 10.1029/96WR02672